Biochemistry and Biophysics Reports 39 (2024) 101789

Contents lists available at ScienceDirect

Biochemistry and Biophysics Reports

journal homepage: www.elsevier.com/locate/bbrep

Expression of opsin and visual cycle-related enzymes in fetal rat skin keratinocytes and cellular response to blue light

Hiroyuki Yamamoto [a,b,*], Momo Okada [b], Yoshikazu Sawaguchi [c], Toshiyuki Yamada [b]

[a] Department of Health and Nutritional Sciences, Faculty of Food and Health Sciences, Aichi Shukutoku University, Nagakute City, Aichi, 480-1197, Japan
[b] Department of Microbiology and Molecular Cell Biology, Nihon Pharmaceutical University, 10281 Komuro, Ina-machi, Kitaadachi-gun, Saitama, 362-0806, Japan
[c] Faculty of Biomedical Engineering, Toin University of Yokohama, Yokohama, Japan

ARTICLE INFO

Keywords:
Opsin
Reninal
Visual cycle
keratinocyte
Cell migration

ABSTRACT

The mechanism by which the skin, a non-visual tissue, responds to light remains unknown. To date, opsin expression has been demonstrated in keratinocytes, melanocytes, and fibroblasts, all of which are skin-derived cells. In this study, we examined whether the visual cycle, by which opsin activity is maintained, is present in skin keratinocytes. We also identified the wavelengths of light to which opsin in keratinocytes responds and explored their effects on skin keratinocytes. The fetal rat skin keratinocytes used in this study expressed OPN2, 3, and 5 in addition to enzymes involved in the visual cycle, and all-*trans*-retinal, which is produced by exposure to light, was reconverted to 11-*cis*-retinal, resulting in opsin activation. Using the production of all-*trans*-retinal after light exposure as an indicator, we discovered that keratinocytes responded to light at 450 nm. Furthermore, actin alpha cardiac muscle 1 expression in keratinocytes was enhanced and cell migration was suppressed by exposure to light at these wavelengths. These results indicate that keratinocytes express various opsins and have a visual cycle that keeps opsin active. Moreover, keratinocytes were shown to respond to the blue/UV region of the light spectrum, suggesting that opsin plays a role in the light response of the skin.

1. Introduction

The response of skin tissue to light is a well-documented phenomenon. Ultraviolet (UV) light, for instance, has a considerable effect on the skin of an organism [1,2], causing protein and DNA denaturation, which leads to wrinkle formation [3], pigmentation [4], and the production of bioactive peptides [5,6]. Several mechanisms by which UV light causes these effects have been reported [7]. UV light modifies proteins and DNA by generating reactive oxygen species, and nucleic acids themselves absorb UV light, causing them to degenerate. The effects of visible light, which has a longer wavelength than UV light, on the skin have also been reported, including on collagen synthesis [8], hyaluronic acid synthesis [9], and melanin production [10,11]. The positive effects of visible light, such as tissue regeneration and pain relief, and the negative effects, such as oxidation and inflammation, are enhanced by violet and blue light, which are also verified by the amount and wavelength of visible light irradiation [12]. Furthermore, it has been shown that the effects of short wavelengths are enhanced by lipofuscin, which increases with UVA dose-dependent [13]. However, the mechanism of the cellular response to visible light is still unclear.

Photopigments are G protein-coupled receptors that are expressed in both visual and non-visual cells [14]. An opsin consists of an apoprotein with a seven-transmembrane structure and the chromophore 11-*cis*-retinal. Genomic studies have identified multiple opsin genes, and opsins are classified into seven groups based on their amino acid sequences. Three types of OPN1 are recognized according to the wavelength that they detect: OPN1-SW, OPN1-MW, and OPN1-LW are sensitive to blue, green, and red light, respectively [15,16]. They are expressed in photoreceptor cells, such as cones and rods, in the optic disc of the retina, playing a role in vision by detecting different wavelengths of light. OPN2, better known as rhodopsin, is also expressed in photoreceptor cells and allows an organism to distinguish between light and dark [17,18]. OPN3, OPN4, and OPN5 are expressed in non-visual cells. OPN3, also known as encephalopsin, is expressed in various tissues, including those in the eye, brain, and liver [19,20], and is activated by light at a wavelength of around 470 nm, which results in a decrease in

Abbreviations: OPN, opsion; UV, Ultraviolet; OLS, Okazaki Large Spectrograph; ActC, actin alpha cardiac muscle 1.

* Corresponding author. Department of Health and Nutritional Sciences, Faculty of Food and Health Sciences, Aichi Shukutoku University, Nagakute 480-1197, Japan.
E-mail address: yamahiro@asu.aasa.ac.jp (H. Yamamoto).

https://doi.org/10.1016/j.bbrep.2024.101789
Received 19 April 2024; Received in revised form 29 June 2024; Accepted 11 July 2024

the intracellular concentration of cyclic adenosine monophosphate (cAMP) [21–23]. OPN4, also called melanopsin, is expressed in retinal ganglion cells and skin tissue [24], and is activated by light at wavelengths of 460–480 nm. The melanopsin is able to drive responses via both Gq and Gi/o, which results in an increase in the intracellular Ca^{2+} concentration and a decrease in the intracellular concentration of cAMP [25,26]. OPN5, also termed neuropsin, is activated by ultraviolet light (360–400 nm wavelength) [27], and its expression has been detected in many neuronal tissues, including the brain and retina [28].

The role of opsins as photopigments in skin cells has been predicted as a mechanism by which the skin receives light [29]. The expression of opsins has also been reported as a mechanism for the photo response of cells derived from skin. Expression of OPN1, 2, 3, and 5 has been reported in keratinocytes [30,31]. OPN1–5 expression has been reported in fibroblasts [32] and melanocytes [31,33], and the expression of OPN1, 3, and 5 is reportedly enhanced by UVA exposure in fibroblasts [34]. OPNs expressed in the skin perform certain functions in response to light exposure. In melanocytes, UV and blue light are involved in the pigmentation process via OPN2, 3, and 4. In fibroblasts, such light exposure is involved in photoaging via OPN3. Moreover, OPN2 is associated with keratinocyte differentiation.

The visual cycle is required for the maintenance of opsin activity, as opsins are apoproteins that require the binding of 11-*cis*-retinal for activation [35–39]. However, upon light exposure, 11-*cis*-retinal is converted to all-*trans*-retinal, which separates from opsin. In the retina, the visual cycle converts all-*trans*-retinal to 11-*cis*-retinal, freeing it to bind to and mature an opsin. In OPN4, which is expressed in endogenous, photosensitive retinal ganglion cells, the photoisomerase retinal G protein-coupled receptor regulates the retinal aldehyde concentration [40].

In this study, we examined whether opsins expressed in keratinocytes and skin tissues are active and whether the visual cycle functions as a mechanism to maintain opsin activity therein. As multiple opsins are expressed in the skin, we expected that a wide range of wavelengths can be received. However, the wavelengths that activate opsins in skin-derived cells are unclear, and we therefore determined this range by using the retinoid metabolism as an indicator. We then explored how cells respond to this wavelength by using proteomic analysis to investigate changes in protein expression after light exposure. In addition, we verified the functions of the proteins that were differentially expressed in keratinocytes.

2. Materials and methods

2.1. Materials

11-*cis*-retinal and 11-*cis*-retinol were purchased from Toronto Research Chemicals (ON, Canada). All-*trans*-retinal and all-*trans*-retinol were purchased from Fujifilm Wako Pure Chemical (Osaka, Japan).

2.2. Cell culture

The FRSK cell line was supplied by Health Science Research Resources Bank (Osaka, Japan). FRSK cells were cultured in DMEM (Nissui Pharmaceutical, Tokyo, Japan) supplemented with 10 % (v/v) fetal bovine serum (Moretate Biotech, Bulimba, Australia) in a humidified atmosphere of 5 % CO_2 and 95 % air at 37 °C. When cells reached 80 % confluency, they were dispersed with 0.05 % (w/v) trypsin in phosphate-buffered saline (PBS) and harvested.

2.3. Animals

All animal experiments were approved by the Animal Experimentation Ethics Committee of Nihon Pharmaceutical University (approval number: 201707) and studies were performed under Nihon Pharmaceutical University guidelines for the use of animals. Additionally, the present study was carried out in compliance with the ARRIVE guidelines. Male Sprague Dawley rats were homebred and housed under standard laboratory conditions (23 ± 1 °C, 55 ± 5 % humidity) with access to tap water and food *ad libitum*. Lights were set to automatically turn on at 08:00 and off at 20:00. After euthanized by decapitation under isoflurane anesthesia, retina and skin tissue were collected.

2.4. Expression of opsins and visual cycle-related genes

The expression of opsins and visual cycle-related genes were assessed using reverse transcription-polymerase chain reaction (RT-PCR). Total RNA was extracted from the FRSK cells, skin and retinas by using TriPure Isolation Reagent (Roche Life Science, Indianapolis, IN, USA), and genomic DNA was removed with DNase I. cDNA was synthesized using ReverTra Ace (Toyobo, Osaka, Japan) according to manufacturer instructions. The primers we used are listed in Table 1. The following PCR cycles were used: initial denaturation at 95 °C for 5 min, followed by 30–40 cycles (depending on the primer) at 94 °C for 1 min, 60 °C for 1 min, and 72 °C for 1 min. PCR products were electrophoresed on ethidium bromide-containing 2 % agarose gels and visualized under UV illumination.

2.5. Sample preparation for SDS-PAGE or western blotting analysis

Extracts of FRSK cells, skin, and retinas were extracted for SDS-PAGE, as follows. The samples were lysed with protein extraction buffer (500 mM Tris–HCl [pH 6.8] and 10 % SDS) and centrifuged at 12,000×*g* at 4 °C for 10 min. The protein concentration of the lysates was measured using the Coomassie Brilliant Blue method, with bovine serum albumin as the standard.

2.6. Western blotting analysis

Samples (10 μg) of the cell lysates were separated on a 12 % (w/v) polyacrylamide gel [41]. Proteins were blotted onto nitrocellulose membranes (Protran BA85; GE Healthcare, Chicago, IL, USA) in a semi-dry blotting system (NA-1513; Nihon Eidoh Co., Tokyo, Japan) [42]. Nitrocellulose membranes were blocked with 2 % (w/v) skim milk in Tris-buffered saline. Blocked membranes were incubated with rabbit anti-ActC antibody (1:10,000; Genetex, Irvine, CA, USA), mouse anti--β-actin monoclonal antibody (1 : 10,000; Fujifilm Wako Pure Chemical, Osaka, Japan) or mouse anti-GAPDH antibody (1:10,000; Fujifilm Wako Pure Chemical, Osaka, Japan). This was followed by incubation with horseradish peroxidase-conjugated goat anti-rabbit immunoglobulin G (IgG) antibody (1:10,000; Seracare, Camarillo, CA, USA) or horseradish peroxidase-conjugated goat anti-mouse IgG antibody (1:3000; Seracare). The blots were subsequently developed using the ImmunoStar Zeta chemiluminescent reagent (Fujifilm Wako Pure Chemical, Osaka, Japan) and a LuminoGraph chemiluminescent imaging system (Atto Corporation, Tokyo, Japan). We subjected the resulting fragments to densitometric analysis using ImageJ software (National Institutes of Health, Bethesda, MD, USA).

2.7. Two-dimensional electrophoresis

We modified the samples by alkylation with 10 mM dithiothreitol and 50 mM monoiodoacetic acid. The modified samples were loaded on a linear ampholyte (GE Healthcare) gradient (pH 4–10) polyacrylamide gel. The electrophoresis was performed overnight by using an increasing voltage (200–1000 V). The gradient gel was placed on the surface of a 12 % (w/v) polyacrylamide gel.

2.8. Silver staining and peptide mass fingerprinting analysis

Silver staining of the gels was performed as previously described, with some modification [43]. Briefly, the gels were fixed with 10 %

(v/v) acetic acid/30 % (v/v) ethanol overnight. After several changes of 20 % (v/v) ethanol and water, the gels were incubated in 0.2 % (w/v) sodium thiosulfate, followed by several washes of water. Thereafter, the gels were incubated in 0.2 % (w/v) silver nitrate and washed briefly with water. Development was performed with 0.01 % (w/v) formaldehyde in 3 % (w/v) sodium bicarbonate and 0.001 % (w/v) sodium thiosulfate. The reaction was stopped with 5 % (w/v) Tris and 2.5 % (v/v) acetic acid. Protein spots were collected and incubated with 15 mM potassium ferricyanide and 50 mM sodium thiosulfate until the color disappeared.

The samples were digested overnight with 10 ng/μl N-tosyl-*L*-phenylalanine chloromethyl ketone-trypsin (Sigma-Aldrich, St. Louis, MO, USA) at 37 °C. For desalting and concentrating, we loaded the digested proteins into ZipTip C18 pipette tips (Millipore, Billerica, MA, USA) and eluted them with 50 % acetonitrile with 0.1 % trifluoroacetic acid. Subsequently, we performed mass spectrometry on a Bruker Autoflex mass spectrometer (Bruker Daltonics, Bremen, Germany). We obtained the spectra in the positive mode and analyzed them with flexAnalysis software (Bruker Daltonics). We used the Mascot program (Matrix Science, London, UK) to conduct database searches.

2.9. Extraction with retinoids

We seeded 3×10^7 FRSK cells in culture dishes. These cells were irradiated with light for 15 min. Retinoid metabolism after light exposure was performed to simultaneous irradiation with LEDs emitting light at wavelengths of 365, 453, 525, 660, 750 and 850 nm. Analysis of the wavelengths of light to which FRSK cells respond was performed using the Okazaki Large Spectrograph at wavelengths of 350, 450, 550, 650 and 750 nm, respectively. Retinals were extracted using the formaldehyde method [44], as follows: 100 μL of 6 M formaldehyde in 0.1 M phosphate buffer was added to the FRSK cells, and incubated at 30 °C for 2 min. After the incubation, 1 mL of dichloromethane was added, and the mixture was vigorously shaken. The mixture was re-incubated at 30 °C for 10 min. Next, 2 mL of *n*-hexane was added and the mixture was shaken. The mixture was centrifuged at 3000 rpm for 5 min and the dichloromethane/*n*-hexane layer was collected. The extraction with dichloromethane/*n*-hexane was repeated once. These extracts were combined and evaporated with centrifugal concentrators. The entire procedure was carried out in a dark room.

Retinols were extracted using hexane [45], as follows: after light irradiation, the FRSK cells were suspended in 0.1 mL of PBS (pH 7.0), after which 0.1 mL of ethanol and 0.4 mL of *n*-hexane were added. The mixture was shaken and subsequently centrifuged at 1000×*g* for 5 min. The *n*-hexane layer was collected. The extraction with *n*-hexane was repeated two times. The extracts were combined and evaporated with centrifugal concentrators. The entire procedure was carried out in a dark room.

2.10. Separation of retinoids via HPLC

The extracted retinals and retinols were dissolved in *n*-hexane. The extracts were combined and analyzed with a Shimadzu HPLC system and a COSMOSIL Cholester column (4.6 mm I.D. × 150 mm; Nacalai Tesque, Inc., Kyoto, Japan). The retinoids were separated at 1 mL/min with 10 % (v/v) methanol and 5 % (v/v) phosphate buffer (pH 2.5) in *n*-hexane, and their absorbances were measured at 340 nm. Retinals and retinols were quantified according to their peak areas with ImageJ software (National Institutes of Health, Bethesda, MD, USA). We performed four independent experiments to measure and analyze retinoids metabolites ratio. Retention time was determined using standard chemicals.

2.11. Wound-healing assay

After growing up to around 90 % confluence in 6-well plates, FRSK cells were treated with LED light (individual exposure at 365, 453, 525, 660, 750, and 850 nm). Cells were scratched with a 200-μL tip and washed with PBS to remove cell debris. We took photos of the scratched areas to record wound widths at the start point (0 h). After cultivation for 24 h, wound widths were photographed at the end point. We measured the scratched areas by using ImageJ software. The migration rates were calculated using the following formula: migration rate (%) = (0-h area −24-h area)/0-h area × 100.

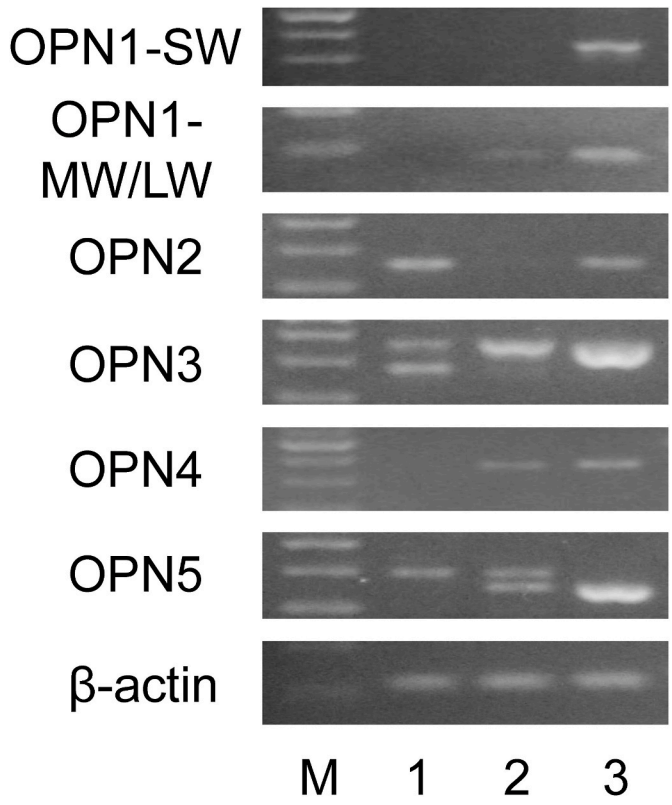

Fig. 1. Expression of opsins in rat skin and rat fetal skin keratinocyte (FRSK) cells
RT-PCR analysis of opsin mRNA expression in rat skin tissue and FRSK cells. M, 1, 2, and 3 represent the DNA size marker, FRSK cells, skin tissue, and retina, respectively.

2.12. Statistical analysis

Data are presented as means ± standard deviations. We analyzed the results via Tukey's tests conducted using R software (version 4.1.2, R Development Core Team, Vienna, Austria), and we considered p-values <0.05 to indicate statistical significance.

3. Results

3.1. Expression of opsins in keratinocytes and skin tissue

We analyzed the expression of opsin in fetal rat skin keratinocyte (FRSK) cells by using RT-PCR (Fig. 1). The retina showed expression of all opsins. OPN1-MW/LW, OPN3, OPN4, and OPN5 mRNA were expressed in skin tissue. Expression of OPN2, OPN3, and OPN5 was observed in FRSK cells. The OPN5 PCR products differed in size between the retinal and skin tissue. OPN3 also exhibited a second PCR product of smaller size in FRSK cells.

3.2. Expression of enzymes related to visual cycle in keratinocytes and skin tissue

We analyzed the expression of enzymes involved in the visual cycle

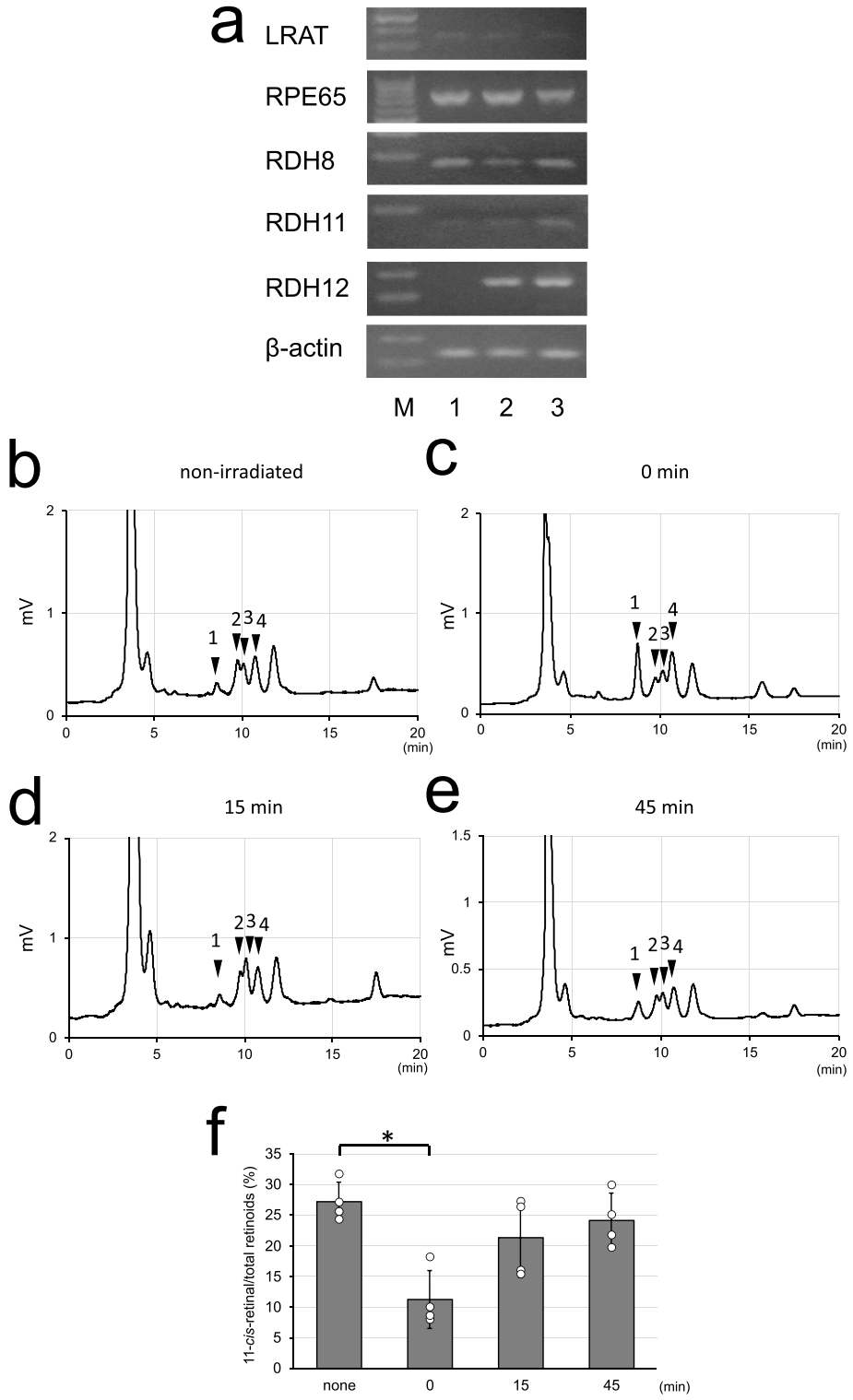

Fig. 2. Visual cycle in rat skin and rat fetal skin keratinocyte (FRSK) cells

RT-PCR analysis of mRNA expression of visual cycle-related enzymes in rat skin tissue and FRSK cells (a). M, 1, 2, and 3 represent the DNA size marker, FRSK cells, skin tissue, and retina, respectively. Chromatogram profiles of retinoids in FRSK cells after simultaneous irradiation with LEDs emitting light at wavelengths of 365, 453, 525, 660, 750, and 850 nm for 15 min (b–e). The light intensity of each wavelength of light was maintained at 1.2–2.7 W/m^2. Numbers 1–4 show the elution positions of the standards for 11-*cis*-retinol, 11-*cis*-retinal, all-*trans*-retinol, and all-*trans*-retinal, respectively. Chromatograms of retinoids extracted from non-irradiated FRSK cells (b), and immediately (c), 15 min (d), and 45 min (e) after irradiation. Ratio of 11-*cis*-retinal to total retinoids in FRSK cells after LED light-irradiation (f). Each bar represents the mean ± standard deviation of four independent experiments. Circles represent individual values from independent experiments. Tukey's multiple comparisons test was performed one-way ANOVA to compare the non-irradiated cells. Asterisks indicate statistical difference between groups.

Table 1
Primer for RT-PCR' should be put near 2.4 Expression of opsins and visual cycle-related genes in the material methods.

Target	Sense primer	Antisense primer
OPN1-SW	TCTTCACAGTCTTCATCGCCAG	CCAGGTATAGTGCTCGCTTC
OPN1-MW/LW	AGCAGAGACCATTATTGCCAGC	GTCCATACAGCAGCCCAGAC
OPN2	CACCTCACTGCATGGCTACTT	ATGGGGATGGTGAAGTGGAC
OPN3	GTCTGGGCGATCTGCTGGTA	ATGCCAAAGAGTAGAGCCAGAT
OPN4	TGGAACAGCACTCAGAACATC	AAAGACAGCCCCACAGAAGG
OPN5	AAGCCTGATTACCATGACTGC	TGGCAATGATCTTCGCGTATG
LRAT	CTCACCTTGCACAGACCAGTTG	AGTTGGAAATAAGGAGCAGC
RPE65	AAGATTAACCCAGAGACCTTG	GCACCATTGACGGAAACATAG
Rdh8	GTGGTGGTCAGCAGTGTTAT	ATTGAACATGACGCCCTGGAG
Rdh11	CAGATGGCTTTGAGATGCAC	CTAGCAGCAAATGGGTCAAGA
Rdh12	TCCATCCGAACCTTTGCTGA	GGAGGTCATGGAAACGGATC
β-actin	AACCCTAAGGCCAACCGTGAAAAG	CGACCAGAGGCATACAGGGACAAC

Table 2
Retention time and ratio of retinal metabolites in rat fetal skin keratinocyte (FRSK) cells after simultaneous exposure to LED at 365, 453, 525, 660, 750, and 850 nm.

	retention time (min)	ratio of retinal metabolites (%)			
		non-irradiated	After irradiated-LED light (min)		
			0	15	45
11-*cis*-retinal	9.6	30.0	12.6	20.9	25.3
11-*cis*-retinol	8.1	44.4	50.8	40.0	38.3
all-*trans*-retinal	11.3	20.8	17.1	26.5	20.1
all-*trans*-retinol	10.2	6.2	19.1	11.3	15.2

The light intensity of each wavelength was maintained at 1.2–2.7 W/m^2. Each result represents the mean of four independent experiments.

via RT-PCR to determine whether a retinoid metabolic pathway is present in the skin and keratinocytes to maintain opsin activity (Fig. 2-a). All the enzymes known to be involved in retinal metabolism were expressed in FRSK cells, with the exception of RDH12.

3.3. Retinol metabolism after light exposure in FRSK cells

The ratios of retinol metabolites after different lengths of light exposure are presented in Table 2. Under our conditions, 11-*cis*-retinal, 11-*cis*-retinol, all-*trans*-retinal, and all-*trans*-retinol were eluted at approximately 9.6, 8.1, 11.3, and 10.2 min, respectively. The experiment was performed after the FRSK cells had been cultured in the dark for at least 6 h; retinoid extraction and analysis were both performed under dark conditions. Retinoids ratio was evaluated four independent experiments. The ratio of 11-*cis*-retinal, all-*trans*-retinal, all-*trans*-retinol, and 11-*cis*-retinol was 30.0 : 44.4: 20.8 : 6.2 (Fig. 2-b). After exactly 15 min of simultaneous exposure to 365 nm, 453 nm, 525 nm, 660 nm, 750 nm, and 850 nm LED light, the ratio was 12.6 : 50.8: 17.1 : 19.1, with a decrease in 11-*cis*-retinal and an increase in the percentage of all-*trans*-retinal (Fig. 2-c). After light exposure was stopped, the ratio at 15 min (Fig. 2-d) and 45 min (Fig. 2-e) was 20.9 : 40.0: 26.5 : 11.3 and 25.3 : 38.3: 20.1 : 15.2, respectively. And then, at approximately 45 min, the values were close to those before light exposure. Light exposure was shown to cause a decrease in the ratio of 11-*cis*-retinal to total retinoids in FRSK cells (Fig. 2-f).

3.4. Wavelength to which FRSK cells respond

We attempted to determine the wavelength of light to which FRSKs respond by monitoring the change in the ratio of retinoids as they were exposed to different wavelengths of light (350, 450, 550, 650, and 750 nm). Using the Okazaki Large Spectrograph, retinoids were extracted immediately after exposure of the keratinocytes to light, and the percentage of 11-*cis*-retinal was evaluated via HPLC (High Performance Liquid Chromatography) elution profiles. Retinoids ratio was measured four independent experiments. Fig. 3-a shows the ratio of 11-*cis*-retinal/all-*trans*-retinal, with smaller values indicating that opsin is activated by the wavelength to which it is exposed. The ratio of 11-*cis*-retinal/all-*trans*-retinal tended to decrease at wavelengths of 350–550 nm, and then significantly decreased at 450 nm. These results suggested that blue/UV opsin responded to light.

3.5. Decrease of ActC expression after blue-light irradiation in FRSK cells

OPN2 [46], OPN3 [22] and OPN5 [27,47] expression in FRSK cells respond to light at 498 nm, 460 nm, and 380 nm, respectively, indicating that they are sensitive to short wavelengths. A response in retinal metabolism was also observed at wavelengths of 350–550 nm. To determine the changes occurring in FRSK cells upon exposure to blue light, proteins with differential expression after 7 days of exposure to a 453 nm blue LED for 15 min per day were analyzed via two-dimensional electrophoresis (Fig. 3-b, c). Some of these proteins exhibited differential expression. The protein circled in Fig. 3-c was identified as actin alpha cardiac muscle 1 (ActC) via peptide mass fingerprinting (Fig. 3-d). Thereafter, the expression of ActC was evaluated via Western blotting (Fig. 3-e, f), which revealed that it was enhanced at wavelengths of 450 nm and 525 nm of blue light. The expression of β-actin and GAPDH was unchanged at all wavelengths (Fig. 3-g).

3.6. Changes in FRSK migration ability at different wavelengths

The suppression of ActC expression in glioblastoma decreases cell migratory ability [48]. Therefore, the effect of exposure to different wavelengths of light on migration ability was evaluated using a wound-healing assay (Fig. 4-a, b). Exposure to light at 365 nm, which corresponds to UV light, suppressed keratinocyte migration to 57 %. In contrast, exposure to wavelengths near 453 nm or 525 nm, at which ActC expression increases, suppressed keratinocyte migration to approximately 20 %.

4. Discussion

In this study, we showed that several types of opsins are expressed in keratinocytes and skin tissue, as OPN2, 3, and 5 were expressed in FRSK cells. OPN5 was detected as two PCR products of different sizes in retina and skin tissue. OPN3 was detected as two PCR products of different sizes in FRSK cells. As previous reports suggested the presence of multiple splicing variants among opsins [31], these multiple PCR products were expected. Several groups have reported the presence of different isoforms of non-visual opsins, some corresponding to substantial changes that occur during fetal and postnatal development [49–51]. In this study, the use of keratinocytes isolated from fetal rats may be the reason that multiple isoforms were detected. However, whether and to what extent OPN3 and OPN5 are active in these cells is unknown. The

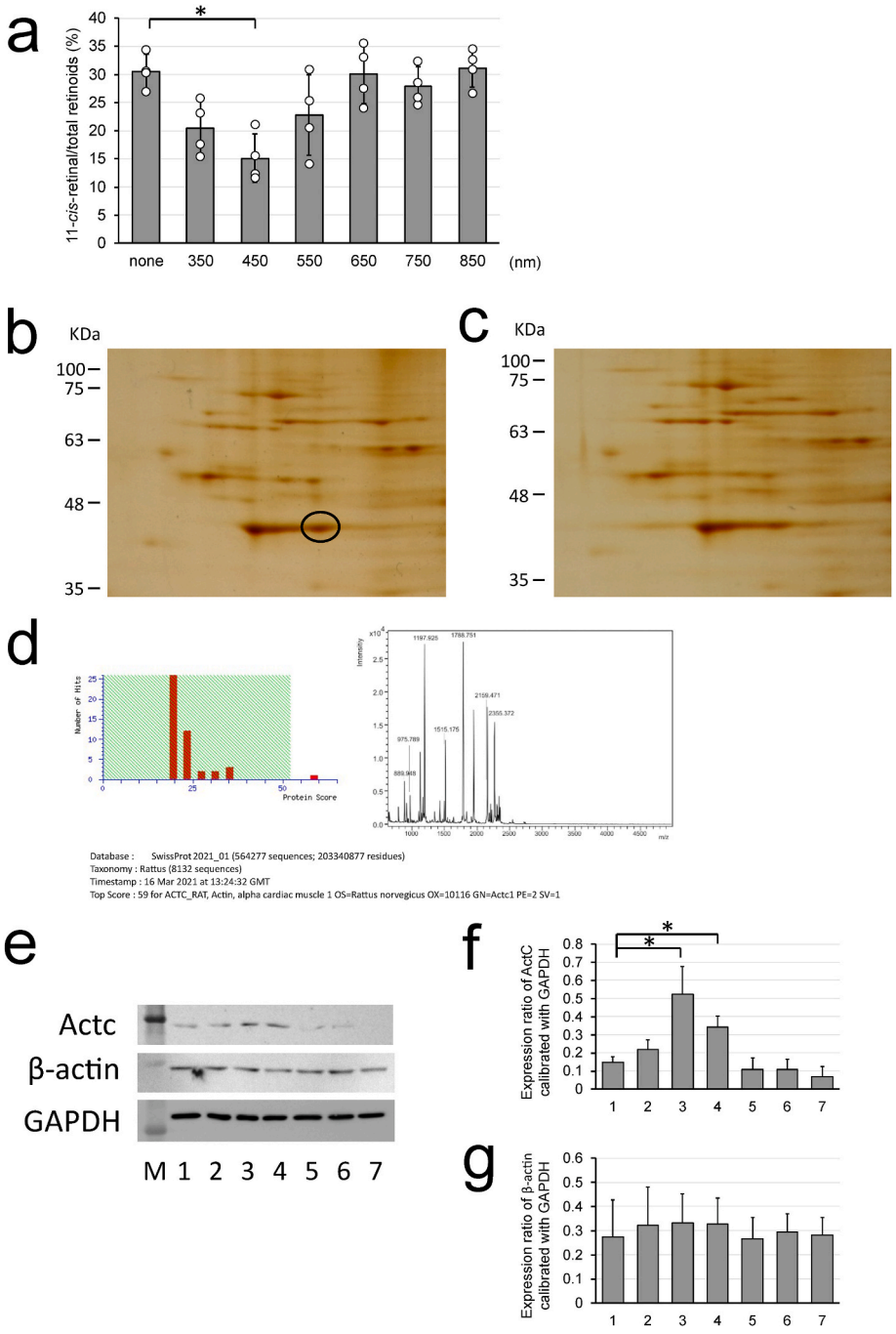

Fig. 3. Response of FRSK cells to exposure to blue light

The ratio of 11-*cis*-retinal in rat fetal skin keratinocyte (FRSK) cells after exposure to light with different wavelengths (350, 450, 550, 650 and 750 nm), evaluated using HPLC elution profiles (a). The irradiated light was spectrally prepared with the Okazaki Large Spectrograph, and the light intensity was maintained at 1.7–2.2 W/m^2. Each bar represents the mean ± standard deviation of four independent experiments. Circles represent individual values from independent experiments. Tukey's multiple comparisons test was performed one-way ANOVA to compare the non-irradiated cells. Asterisks indicate statistical difference between groups. Extracts from FRSK cells that had been exposed to LED light at a wavelength of 453 nm for 15 min per day (b) or those from non-irradiated cells (c) were separated with two-dimensional electrophoresis. The circled spot was used for peptide mass fingerprinting. Mass spectra of trypsin-digested fragments, along with the search results in the Mascot program (d). The spot was identified a match for rat ActC by peptide mass fingerprinting analysis, with a significant score of 59 ($p = 0.011$). Sequence coverage was 29 %. Western blot analysis for the expression of ActC, β-actin, and GAPDH in FRSK cells after exposure to LED light at 365–850 nm (e). β-actin and GAPDH were used as controls. The ActC (f) and β-actin (g) density was measured using ImageJ software, calibrated against GAPDH. Results show the mean ± standard deviation of at least three independent experiments. Tukey's multiple comparisons test was performed one-way ANOVA to compare the non-irradiated cells. Asterisks indicate statistical difference between groups. M, 1, 2, 3, 4, 5, 6, and 7 represent the protein size marker, non-irradiated cells, and cells irradiated with LED light at 365 nm, 453 nm, 525 nm, 660 nm, 750 nm, and 850 nm, respectively. (For interpretation of the references to color in this figure legend, the reader is referred to the Web version of this article.)

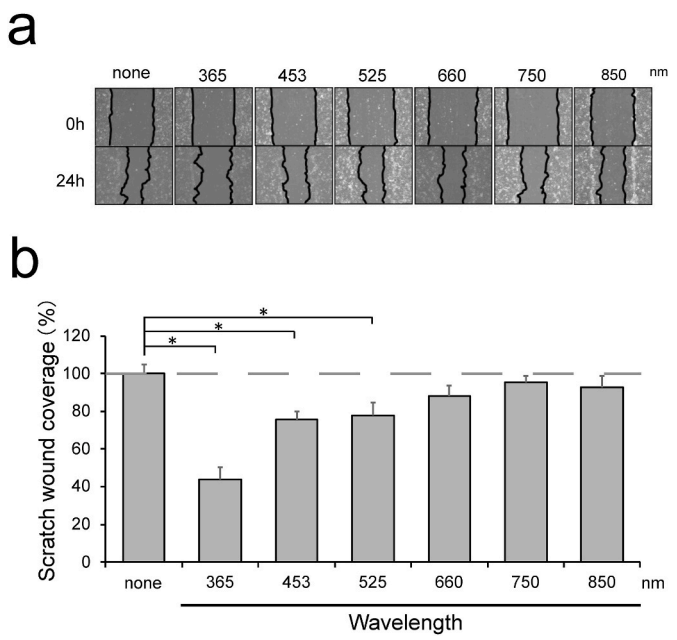

Fig. 4. Migratory ability of rat fetal skin keratinocyte (FRSK) cells altered by exposure to light of various wavelengths
Effect of exposure to LED lights at different wavelengths (365, 453, 525, 660, 750, and 850 nm) on the wound-healing of FRSK cells. The light intensity of each wavelength was maintained at 1.2–2.7 W/m^2. Bright-field images of the scratched area of FRSK cells at 0 and 24 h after scratching (a). Wound closure was 100 % for non-irradiated FRSK cells (b). Each bar represents the mean ± standard deviation of at least three independent experiments. Tukey's multiple comparisons test was performed one-way ANOVA to compare the non-irradiated cells. Asterisks indicate statistical difference between groups.

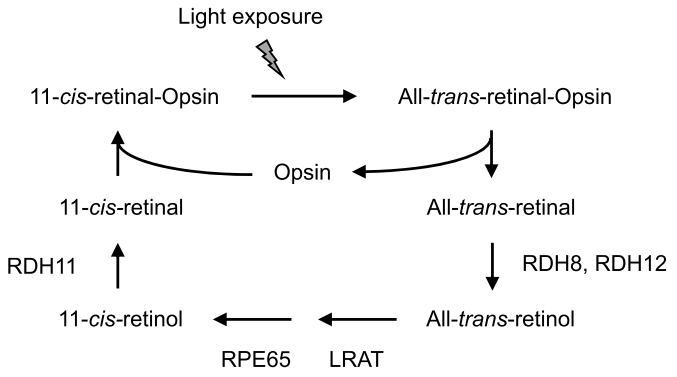

Fig. 5. Visual cycle and related enzymes.

peak response of OPN2, 3, and 5 expression in FRSK cells was previously detected at 498 nm, 460 nm, and 380 nm, respectively [22,27,46,47], suggesting that they are all activated by short-wavelength blue light.

Next, we evaluated the presence of a visual cycle in FRSK cells, which is required for the maintenance of opsin function. In that cycle, all-*trans*-retinal is converted again to 11-*cis*-retinal by the RDH8, RDH12, RPE65, LRAT, and RDH11 enzymes and binds to opsin to activate it in the retina [38,39]. All of these enzymes were expressed in rat skin in this study, and only RDH12 expression was not detected in FRSK cells. In general, in the visual cycle (Fig. 5), RDH8 and RDH12 are both responsible for the conversion of all-*trans*-retinal to all-*trans*-retinol [52–54]. Therefore, our results suggest that RDH8 is responsible for this conversion in FRSK cells. Our results also indicate that in skin tissues and keratinocytes can convert all-*trans*-retinal to 11-*cis*-retinal in the visual cycle.

Subsequently, we tested whether the visual cycle is functional in FRSK cells by measuring retinoid metabolites after light exposure. The amount of 11-*cis*-retinal decreased after light exposure, indicating that opsin expressed in FRSK cells was responsive to light. After 45 min, the amount of 11-*cis*-retinal was at the same level as before light exposure, suggesting that this is the time required for the resynthesis of 11-*cis*-retinal.

Next, detection of retinoid metabolites after light exposure revealed that FRSK cells respond to blue light. We demonstrated that the blue light to which FRSK cells respond enhances ActC expression and suppresses cell migration. ActC is an actin expressed in mature heart and fetal skeletal muscle and has a high homology with ActA and ActB [55]. Actin is an important protein in the formation of the cytoskeleton and generates physical forces such as cell migration; ActC is also involved in cell migration [56], and suppression of ActC expression in glioblastoma reportedly reduces cell migratory ability [48]. In other words, migration ability in glioblastoma is enhanced by ActC. In contrast, we discovered that an increase in ActC induced by exposure to blue light decreased cell migration in FRSK cells. The cause of the difference in the effect of increased ActC on cell migration ability is unknown. Exposure to blue light reportedly decreases the migratory ability of keratinocytes, supporting the results of this experiment [57]. Vinculin reportedly migrates to the cell membrane in melanocytes upon UVA or UVB exposure [58,59]. It is also known to be involved in the formation of cell adhesion plaques and the regulation of cell migration [60,61], and a similar mechanism may be in place in FRSK cells. As β-actin was expressed, the ratio of ActC to β-actin expression may alter the speed of actin filament formation and filament strength, thereby affecting keratinocyte migration. The fact that ActC expression is decreased at longer wavelengths of light (650–850 nm) without affecting migration ability also indicates that the constant expression of β-actin is sufficient for cell migration. In this study, we did not perform gene knockout/silencing experiments of ActC. Therefore, we could not rule out that the reduction of cell migration by blue light is mediated by a factor other than ActC. The cause of this phenomenon is unknown and requires verification in future research.

In conclusion, the present study demonstrates that opsins and enzymes involved in the visual cycle are expressed in skin keratinocytes. Moreover, all-*trans*-retinal, which is produced after light exposure, is converted back to 11-*cis*-retinal via the visual cycle, keeping opsins active. Using retinoid metabolism as an indicator, we also showed that keratinocytes respond to light at wavelengths around 450 nm by increasing ActC expression and inhibiting cell migration. These results indicate that non-visual cells recognize violet/blue light and exhibit a cellular response, suggesting that opsin is involved in maintaining skin homeostasis after light exposure.

Funding

This work was supported by funding from the KOSÉ Cosmetology Research Foundation to HY and by JSPS KAKENHI (grant numbers: JP23K05029 and JP20K05829) to HY.

CRediT authorship contribution statement

Hiroyuki Yamamoto: Writing – review & editing, Writing – original draft, Investigation, Funding acquisition, Conceptualization. **Momo Okada:** Investigation. **Yoshikazu Sawaguchi:** Writing – review & editing, Investigation. **Toshiyuki Yamada:** Writing – review & editing, Investigation.

Declaration of competing interest

The authors declare that they have no known competing financial interests or personal relationships that could have appeared to influence the work reported in this paper.

Acknowledgments

This work was supported by the NIBB Collaborative Research Experiment for the Okazaki Large Spectrograph (20–607, 21–502, 22NIBB603, and 23NIBB601) to HY. We thank Prof. Yasuhiro Kamei for valuable discussions of this experiment.

Appendix A. Supplementary data

Supplementary data to this article can be found online at https://doi.org/10.1016/j.bbrep.2024.101789.

References

[1] A.R. Young, C.A. Chadwick, G.I. Harrison, O. Nikaido, J. Ramsden, C.S. Potten, The similarity of action spectra for thymine dimers in human epidermis and erythema suggests that DNA is the chromophore for erythema, J. Invest. Dermatol. 111 (1998) 982–988, https://doi.org/10.1046/j.1523-1747.1998.00436.x.

[2] J.A. Parrish, K.F. Jaenicke, R.R. Anderson, Erythema and melanogenesis action spectra of normal human skin, Photochem. Photobiol. 36 (1982) 187–191, https://doi.org/10.1111/j.1751-1097.1982.tb04362.x.

[3] D.L. Bissett, R. Chatterjee, D.P. Hannon, Photoprotective effect of topical anti-inflammatory agents against ultraviolet radiation-induced chronic skin damage in the hairless mouse, Photodermatol. Photoimmunol. Photomed. 7 (1990) 153–158.

[4] W. Montagna, K. Carlisle, The architecture of black and white facial skin, J. Am. Acad. Dermatol. 24 (1991) 929–937, https://doi.org/10.1016/0190-9622(91)70148-u.

[5] H. Yamamoto, T. Yamane, K. Iguchi, K. Tanaka, A. Iddamalgoda, K. Unno, M. Hoshino, A. Takeda, Melanin production through novel processing of proopiomelanocortin in the extracellular compartment of the auricular skin of C57BL/6 mice after UV-irradiation, Sci. Rep. 5 (2015) 14579, https://doi.org/10.1038/srep14579.

[6] H. Yamamoto, N. Wakamatsu, R. Yanagisawa, K. Iguchi, Expression of prosecretin in the keratinocyte after UV-irradiation, Biochem. Cell. Arch. 20 (2020) 1–7.

[7] J. D'Orazio, S. Jarrett, A. Amaro-Ortiz, T. Scott, UV radiation and the skin, Int. J. Mol. Sci. 14 (2013) 12222–12248, https://doi.org/10.3390/ijms140612222.

[8] D. Barolet, C.J. Roberge, F.A. Auger, A. Boucher, L. Germain, Regulation of skin collagen metabolism in vitro using a pulsed 660 nm LED light source: clinical correlation with a single-blinded study, J. Invest. Dermatol. 129 (2009) 2751–2759, https://doi.org/10.1038/jid.2009.186.

[9] S. Moriwaki, S. Kawamata, M. Kotani, A. Fujita, T. Hirano, Effect of red light emitting diodes (LED) on human dermal fibroblasts, Aesthetic Dermatology 18 (2008) 30–34.

[10] J.M. Kim, N.H. Kim, Y.S. Tian, A.Y. Lee, Light-emitting diodes at 830 and 850 nm inhibit melanin synthesis in vitro, Acta Derm. Venereol. 92 (2012) 675–680, https://doi.org/10.2340/00015555-1319.

[11] C.T. Oh, T.R. Kwon, E.J. Choi, S.R. Kim, J. Seok, S.K. Mun, K.H. Yoo, Y.S. Choi, S. Y. Choi, B.J. Kim, Inhibitory effect of 660-nm LED on melanin synthesis in in vitro and in vivo, Photodermatol. Photoimmunol. Photomed. 33 (2017) 49–57, https://doi.org/10.1111/phpp.12276.

[12] P.N. Tonolli, C.M. Vera Palomino, H.C. Junqueira, M.S. Baptista, The phototoxicity action spectra of visible light in HaCaT keratinocytes, J. Photochem. Photobiol., B 243 (2023) 112703, https://doi.org/10.1016/j.jphotobiol.2023.112703.

[13] P.N. Tonolli, O. Chiarelli-Neto, C. Santacruz-Perez, H.C. Junqueira, I.S. Watanabe, F.G. Ravagnani, W.K. Martins, M.S. Baptista, Lipofuscin generated by UVA turns keratinocytes photosensitive to visible light, J. Invest. Dermatol. 137 (2017) 2447–2450, https://doi.org/10.1016/j.jid.2017.06.018.

[14] A. Terakita, The opsins, Genome Biol. 6 (2005) 213, https://doi.org/10.1186/gb-2005-6-3-213.

[15] J. Nathans, D.S. Hogness, Isolation and nucleotide sequence of the gene encoding human rhodopsin, Proc Natl Acad Sci U S A. 81 (1984) 4851–4855, https://doi.org/10.1073/pnas.81.15.4851.

[16] J. Nathans, D. Thomas, D.S. Hogness, Molecular genetics of human color vision: the genes encoding blue, green, and red pigments, Science 232 (1986) 193–202, https://doi.org/10.1126/science.2937147.

[17] P.A. Hargrave, J.H. McDowell, D.R. Curtis, J.K. Wang, E. Juszczak, S.L. Fong, J. K. Rao, P. Argos, The structure of bovine rhodopsin, Biophys. Struct. Mech. 9 (1983) 235–244, https://doi.org/10.1007/bf00535659.

[18] L.A. Drachev, G.R. Kalamkarov, A.D. Kaulen, M.A. Ostrovsky, V.P. Skulachev, Animal rhodopsin as a photogenerator of an electric potential that increases photoreceptor membrane permeability, FEBS Lett. 119 (1980) 125–131, https://doi.org/10.1016/0014-5793(80)81013-1.

[19] S. Blackshaw, S.H. Snyder, Encephalopsin: a novel mammalian extraretinal opsin discretely localized in the brain, J. Neurosci. 19 (1999) 3681–3690, https://doi.org/10.1523/jneurosci.19-10-03681.1999.

[20] G. Kasper, S. Taudien, E. Staub, D. Mennerich, M. Rieder, B. Hinzmann, E. Dahl, U. Schwidetzky, A. Rosenthal, A. Rump, Different structural organization of the encephalopsin gene in man and mouse, Gene 295 (2002) 27–32, https://doi.org/10.1016/s0378-1119(02)00799-0.

[21] S. Halford, M.S. Freedman, J. Bellingham, S.L. Inglis, S. Poopalasundaram, B. G. Soni, R.G. Foster, D.M. Hunt, Characterization of a novel human opsin gene with wide tissue expression and identification of embedded and flanking genes on chromosome 1q43, Genomics 72 (2001) 203–208, https://doi.org/10.1006/geno.2001.6469.

[22] T. Sugihara, T. Nagata, B. Mason, M. Koyanagi, A. Terakita, Absorption Characteristics of vertebrate non-visual opsin, Opn3, PLoS One 11 (2016) e0161215, https://doi.org/10.1371/journal.pone.0161215.

[23] M. Koyanagi, E. Takada, T. Nagata, H. Tsukamoto, A. Terakita, Homologs of vertebrate Opn3 potentially serve as a light sensor in nonphotoreceptive tissue, Proc Natl Acad Sci U S A 110 (2013) 4998–5003, https://doi.org/10.1073/pnas.1219416110.

[24] I. Provencio, G. Jiang, W.J. De Grip, W.P. Hayes, M.D. Rollag, Melanopsin: an opsin in melanophores, brain, and eye, Proc Natl Acad Sci U S A. 95 (1998) 340–345, https://doi.org/10.1073/pnas.95.1.340.

[25] M. Hatori, S. Panda, The emerging roles of melanopsin in behavioral adaptation to light, Trends Mol. Med. 16 (2010) 435–446, https://doi.org/10.1016/j.molmed.2010.07.005.

[26] H.J. Bailes, R.J. Lucas, Human melanopsin forms a pigment maximally sensitive to blue light (λmax ≈ 479 nm) supporting activation of G(q/11) and G(i/o) signalling cascades, Proc. Biol. Sci. 280 (2013) 20122987, https://doi.org/10.1098/rspb.2012.2987.

[27] D. Kojima, S. Mori, M. Torii, A. Wada, R. Morishita, Y. Fukada, UV-sensitive photoreceptor protein OPN5 in humans and mice, PLoS One 6 (2011) e26388, https://doi.org/10.1371/journal.pone.0026388.

[28] J. Suzuki, S. Yoshida, Z.L. Chen, Y. Momota, K. Kato, A. Hirata, S. Shiosaka, Ontogeny of neuropsin mRNA expression in the mouse brain, Neurosci. Res. 23 (1995) 345–351, https://doi.org/10.1016/0168-0102(95)00960-2.

[29] S. Suh, E.H. Choi, N. Atanaskova Mesinkovska, The expression of opsins in the human skin and its implications for photobiomodulation: a Systematic Review, Photodermatol. Photoimmunol. Photomed. 36 (2020) 329–338, https://doi.org/10.1111/phpp.12578.

[30] M. Tsutsumi, K. Ikeyama, S. Denda, J. Nakanishi, S. Fuziwara, H. Aoki, M. Denda, Expressions of rod and cone photoreceptor-like proteins in human epidermis, Exp. Dermatol. 18 (2009) 567–570, https://doi.org/10.1111/j.1600-0625.2009.00851.x.

[31] K. Haltaufderhyde, R.N. Ozdeslik, N.L. Wicks, J.A. Najera, E. Oancea, Opsin expression in human epidermal skin, Photochem. Photobiol. 91 (2015) 117–123, https://doi.org/10.1111/php.12354.

[32] Y. Lan, H. Lu, Opsin expression in human dermis fibroblasts in vitro, J. Invest. Dermatol. 138 (2018) S189.

[33] N.L. Wicks, J.W. Chan, J.A. Najera, J.M. Ciriello, E. Oancea, UVA phototransduction drives early melanin synthesis in human melanocytes, Curr. Biol. 21 (2011) 1906–1911, https://doi.org/10.1016/j.cub.2011.09.047.

[34] Y. Lan, Y. Wang, H. Lu, Opsin 3 is a key regulator of ultraviolet A-induced photoageing in human dermal fibroblast cells, Br. J. Dermatol. 182 (2020) 1228–1244, https://doi.org/10.1111/bjd.18410.

[35] R. Hubbard, G. Wald, Cis-trans isomers of vitamin A and retinene in the rhodopsin system, J. Gen. Physiol. 36 (1952) 269–315, https://doi.org/10.1085/jgp.36.2.269.

[36] G. Wald, P.K. Brown, Human rhodopsin, Science. 127 (1958) 222–226, https://doi.org/10.1126/science.127.3292.222.

[37] G.W. Stubbs, J.C. Saari, S. Futterman, 11-cis-Retinal-binding protein from bovine retina. Isolation and partial characterization, J. Biol. Chem. 254 (1979) 8529–8533.

[38] M. Jin, S. Li, W.N. Moghrabi, H. Sun, G.H. Travis, Rpe65 is the retinoid isomerase in bovine retinal pigment epithelium, Cell 122 (2005) 449–459, https://doi.org/10.1016/j.cell.2005.06.042.

[39] G. Moiseyev, Y. Chen, Y. Takahashi, B.X. Wu, J.X. Ma, RPE65 is the isomerohydrolase in the retinoid visual cycle, Proc Natl Acad Sci U S A 102 (2005) 12413–12418, https://doi.org/10.1073/pnas.0503460102.

[40] M.E. Guido, N.A. Marchese, M.N. Rios, L.P. Morera, N.M. Diaz, E. Garbarino-Pico, M.A. Contin, Non-visual opsins and novel photo-Detectors in the vertebrate Inner retina mediate light responses within the blue spectrum region, Cell. Mol. Neurobiol. 42 (2022) 59–83, https://doi.org/10.1007/s10571-020-00997-x.

[41] U.K. Laemmli, Cleavage of structural proteins during the assembly of the head of bacteriophage T4, Nature 227 (1970) 680–685, https://doi.org/10.1038/227680a0.

[42] W.N. Burnette, "Western blotting": electrophoretic transfer of proteins from sodium dodecyl sulfate–polyacrylamide gels to unmodified nitrocellulose and radiographic detection with antibody and radioiodinated protein A, Anal. Biochem. 112 (1981) 195–203, https://doi.org/10.1016/0003-2697(81)90281-5.

[43] C.R. Merril, R.C. Switzer, M.L. Van Keuren, Trace polypeptides in cellular extracts and human body fluids detected by two-dimensional electrophoresis and a highly sensitive silver stain, Proc Natl Acad Sci U S A. 76 (1979) 4335–4339, https://doi.org/10.1073/pnas.76.9.4335.

[44] T. Suzuki, Y. Fujita, Y. Noda, S. Miyata, A simple procedure for the extraction of the native chromophore of visual pigments: the formaldehyde method, Vision Res. 26 (1986) 425–429, https://doi.org/10.1016/0042-6989(86)90185-9.

[45] J. Weng, N.L. Mata, S.M. Azarian, R.T. Tzekov, D.G. Birch, G.H. Travis, Insights into the function of Rim protein in photoreceptors and etiology of Stargardt's disease from the phenotype in abcr knockout mice, Cell 98 (1999) 13–23, https://doi.org/10.1016/s0092-8674(00)80602-9.

[46] H.J. Dartnall, J.K. Bowmaker, J.D. Mollon, Human visual pigments: microspectrophotometric results from the eyes of seven persons, Proc. R. Soc. Lond. B Biol. Sci. 220 (1983) 115–130, https://doi.org/10.1098/rspb.1983.0091.

[47] T. Yamashita, K. Ono, H. Ohuchi, A. Yumoto, H. Gotoh, S. Tomonari, K. Sakai, H. Fujita, Y. Imamoto, S. Noji, K. Nakamura, Y. Shichida, Evolution of mammalian

Opn5 as a specialized UV-absorbing pigment by a single amino acid mutation, J. Biol. Chem. 289 (2014) 3991–4000, https://doi.org/10.1074/jbc.M113.514075.
[48] M. Wanibuchi, S. Ohtaki, S. Ookawa, Y. Kataoka-Sasaki, M. Sasaki, S. Oka, Y. Kimura, Y. Akiyama, T. Mikami, N. Mikuni, J.D. Kocsis, O. Honmou, Actin, alpha, cardiac muscle 1 (ACTC1) knockdown inhibits the migration of glioblastoma cells in vitro, J. Neurol. Sci. 392 (2018) 117–121, https://doi.org/10.1016/j.jns.2018.07.013.
[49] J. Bellingham, S.S. Chaurasia, Z. Melyan, C. Liu, M.A. Cameron, E.E. Tarttelin, P. M. Iuvone, M.W. Hankins, G. Tosini, R.J. Lucas, Evolution of melanopsin photoreceptors: discovery and characterization of a new melanopsin in nonmammalian vertebrates, PLoS Biol. 4 (2006) e254, https://doi.org/10.1371/journal.pbio.0040254.
[50] D.M. Verra, M.A. Contín, D. Hicks, M.E. Guido, Early onset and differential temporospatial expression of melanopsin isoforms in the developing chicken retina, Invest. Ophthalmol. Vis. Sci. 52 (2011) 5111–5120, https://doi.org/10.1167/iovs.11-75301.
[51] M.N. Rios, N.A. Marchese, M.E. Guido, Expression of non-visual opsins Opn3 and Opn5 in the developing Inner retinal cells of Birds. Light-responses in Müller glial cells, Front. Cell. Neurosci. 13 (2019) 376, https://doi.org/10.3389/fncel.2019.00376.
[52] A. Rattner, P.M. Smallwood, J. Nathans, Identification and characterization of all-trans-retinol dehydrogenase from photoreceptor outer segments, the visual cycle enzyme that reduces all-trans-retinal to all-trans-retinol, J. Biol. Chem. 275 (2000) 11034–11043, https://doi.org/10.1074/jbc.275.15.11034.
[53] F. Haeseleer, G.F. Jang, Y. Imanishi, C. Driessen, M. Matsumura, P.S. Nelson, K. Palczewski, Dual-substrate specificity short chain retinol dehydrogenases from the vertebrate retina, J. Biol. Chem. 277 (2002) 45537–45546, https://doi.org/10.1074/jbc.M208882200.
[54] A. Maeda, K. Palczewski, Retinal degeneration in animal models with a defective visual cycle, Drug Discov Today Dis Models 10 (2013) e163–e172, https://doi.org/10.1016/j.ddmod.2014.01.001.
[55] B. Ilkovski, S. Clement, C. Sewry, K.N. North, S.T. Cooper, Defining alpha-skeletal and alpha-cardiac actin expression in human heart and skeletal muscle explains the absence of cardiac involvement in ACTA1 nemaline myopathy, Neuromuscul. Disord. 15 (2005) 829–835, https://doi.org/10.1016/j.nmd.2005.08.004.
[56] S. Ohtaki, M. Wanibuchi, Y. Kataoka-Sasaki, M. Sasaki, S. Oka, S. Noshiro, Y. Akiyama, T. Mikami, N. Mikuni, J.D. Kocsis, O. Honmou, ACTC1 as an invasion and prognosis marker in glioma, J. Neurosurg. 126 (2017) 467–475, https://doi.org/10.3171/2016.1.Jns152075.
[57] M. Denzinger, M. Held, S. Krauss, C. Knorr, C. Memmel, A. Daigeler, W. Eisler, Does Phototherapy Promote wound healing? Limitations of blue light irradiation, Wounds 33 (2021) 91–98.
[58] H. Yamamoto, H. Yamaguchi, T. Yamada, Vinculin migrates to the cell membrane of melanocytes after UVB irradiation, BPB Reports 3 (2020) 126–129, https://doi.org/10.1248/bpbreports.3.4_126.
[59] H. Yamamoto, C. Tanaka, M. Okada, Y. Sawaguchi, T. Yamada, Membrane translocation of vinculin after UVA exposure facilitates melanosome trafficking, Drug Discov Ther 16 (2022) 293–296, https://doi.org/10.5582/ddt.2022.01075.
[60] B. Geiger, K.T. Tokuyasu, A.H. Dutton, S.J. Singer, Vinculin, an intracellular protein localized at specialized sites where microfilament bundles terminate at cell membranes, Proc Natl Acad Sci U S A 77 (1980) 4127–4131, https://doi.org/10.1073/pnas.77.7.4127.
[61] J.L. Bays, K.A. DeMali, Vinculin in cell-cell and cell-matrix adhesions, Cell. Mol. Life Sci. 74 (2017) 2999–3009, https://doi.org/10.1007/s00018-017-2511-3.